Effect of Polarizability on the Potential of Mean Force of Two Cations. The Guanidinium−Guanidinium Ion Pair in Water

Jean-Christophe Soetens,[†,‡] Claude Millot,[*,†] Christophe Chipot,[†] Georg Jansen,[‡] János G. Ángyán,[†] and Bernard Maigret[†]

Laboratoire de Chimie Théorique, Université Henri-Poincaré-Nancy I, Unité de Recherche Associée au CNRS no 510, BP 239, 54506 Vandoeuvre-lès-Nancy Cedex, France, and Institut für Theoretische Chemie, Heinrich-Heine Universität Düsseldorf, Universitätsstrasse 1, D-40225 Düsseldorf, Germany

Received: July 1, 1997; In Final Form: September 24, 1997[⊗]

The potential of mean force of two rigid guanidinium ions constrained to remain parallel is investigated in liquid water by means of free energy perturbation (FEP) molecular dynamics simulations, using various intermolecular potentials. The first simulation is carried out employing the Amber force field and the transferable intermolecular potential TIP3P water model. The second simulation is performed with the extended simple point charge SPC/E water model. In a third simulation, the polarizability of the water molecule is introduced via the use of the polarizable simple point charge model PSPC, whereas for the ions, distributed polarizabilities derived from the topological partitioning of electrostatic properties (TPEP) are incorporated on heavy atoms. For the last two simulations, atom−atom Lennard-Jones parameters and charges are derived from ab initio calculations on monomers and guanidinium−water pairs. The comparison with a previous simulation using the transferable intermolecular potential TIP4P, by Boudon et al. (*J. Phys. Chem.* **1990**, *94*, 6056−61), reveals that (i) all the models predict a stable contact ion pair (CIP) at a distance of 3.0−3.4 Å, and a solvent-separated ion pair (SSIP) at about 6.5 Å, (ii) the stabilization energy of the CIP is strongly model-dependent, varying from 10.0 kcal·mol^{-1}, for the TIP4P model to 4.7 and 2.7 kcal·mol^{-1} for the SPC/E and PSPC models respectively, and (iii) in all cases, the SSIP free energy minimum is very shallow and nearly disappears for the simulation using a polarizable model. Consideration of the distribution and the orientation of the solvent molecules around the ions for the non-polarizable (SPC/E) and the polarizable (PSPC) cases does not reveal any significant difference between the two models.

1. Introduction

Molecular dynamics (MD) and Monte Carlo (MC) simulations are nowadays employed routinely to investigate ion association in liquid phases. Whereas many studies have dealt with simple atomic ions in water, molecular ions[1−3] and other solvents[4−7] have also been considered. These studies, undertaken via computer simulation, usually focus on the potential of mean force (PMF) of an ion pair. In addition, the solvent structure around the ions can be analyzed together with the dynamics of dissociation of the ion pair.[8,9]

Several studies have been carried out on monoatomic ions of identical charges or opposite charges. They have highlighted the sensitivity of the results to the force field parameters, the treatment of long range interactions, as well as other simulation features. In addition, a comparison with the prediction obtained from methods based upon integral equations has led to controversies, especially for like-charge ion pairs, e.g. the Cl^-−Cl^- pair.[3,10−12]

An interesting issue in this field is the correct treatment of polarization effects of the solvent. When ions are solvated, the solvent molecules are significantly polarized in the first shells and the use of effective potentials is arguable. This remark is particularly relevant for an aqueous medium, in which the water molecules are small and noticeably polarizable. Some studies have indicated that the explicit inclusion of the polarizability of water in the intermolecular potential has a significant effect on the Cl^-−Cl^- PMF. Van Belle and Wodak[13] have also found significant differences for the methane−methane PMF in polarizable and non- polarizable water. New and Berne[14] have reconsidered the same system and have found, in contradiction with Van Belle and Wodak, that using a polarizable water model increases the stability of the solvent separated pair with respect to the contact pair.

Here, we investigate the PMF of the guanidinium ion pair in bulk water. This system can be regarded as a model of a pair of positively charged arginine side chains, which can be observed in many proteins, in particular in their solvent accessible regions. Such pairs have proven to play a significant role in the structure and the stability of proteins.[15] It has been found[16] that more than 40 proteins in the Brookhaven protein structural data bank[17,18] have arginine pairs in parallel planes with charged terminations separated by less than 5.0 Å. It would, thus, be instructive to confirm and understand the reasons of the stability of such like-charge ion pairs at short distances. A few years ago, Boudon et al.[19] have computed the guanidinium−guanidinium PMF in TIP4P water and have shown the existence of a 10 kcal·mol^{-1} deep free energy minimum, located at an interionic distance of 3.4 Å. A number of studies of the Cl^-−Cl^- ion pair in various water models (e.g., TIP4P, SPC, flexible SPC) has revealed that the generated PMF is very model-dependent and that the TIP4P model is unique in predicting a stable contact ion pair.[3] This situation has led us to reinvestigate the guanidinium−guanidinium case with the TIP3P[20] and the SPC/E[21] effective water models. Furthermore, we will examine the effect of the solvent polarizability on the PMF. Toward this end, we have employed the PSPC[22] model, a polarizable model derived, just like SPC/E from the SPC[23] effective model.

[†] Université Henri Poincaré.
[‡] Heinrich-Heine Universität Düsseldorf.
[⊗] Abstract published in *Advance ACS Abstracts,* November 15, 1997.

S1089-5647(97)02113-5 CCC: $14.00

TABLE 1: Compilation of the Different Types of Models Considered

type	water models	guanidinium models
nonpolarizable	TIP4P[20]	RHF/6-31G(d) potential derived charges + LJ parameters fitted to RHF/6-31G(d) optimized dimers
nonpolarizable	TIP3P[20]	RHF/6-31G** potential derived charges + LJ parameters of Amber force field + H-bond ion−water 10−12 term
nonpolarizable	SPC/E[21]	RHF/6-31G** potential derived charges + LJ parameters fitted to RHF/6-31G(d) optimized dimers
polarizable	PSPC[22]	MP2/6-311++G** potential derived charges + TPEP charge flux and local dipolar polarizabilities + LJ parameters fitted to MP2/6-311++G** optimized dimers

TABLE 2: Nonbonded Parameters for the Guanidinium Ion Used in Our Different MD Simulations with Respect to the Solvent Water Models[d]

		van der Waals parameters		
water models	atoms	(Å)	(kcal·mol^{-1})	charges (e)
TIP3P[a,b]		r^*_{ii}	ϵ_{ii}	q
	C	3.70	0.1200	1.0957
	N	3.50	0.1600	−1.0163
	H	2.00	0.0200	0.4922
SPC/E[c]		σ_{ii}	ϵ_{ii}	q
	C	2.25	0.1200	1.0957
	N	3.41	0.1600	−1.0163
	H			0.4922
PSPC[c]		σ_{ii}	ϵ_{ii}	q
	C	2.25	0.0502	1.0000
	N	3.20	0.1575	−0.9800
	H	1.40	0.0406	0.4900

[a] The mixing rules are $r^*_{ij} = (r^*_{ii} + r^*_{jj})/2$ and $\epsilon_{ij} = (\epsilon_{ii}\epsilon_{jj})^{1/2}$. [b] This model uses also an $H_{(ion)}-O_{(water)}$ 10−12 term with the following parameters: $C = 7557$ kcal·Å^{12}·mol^{-1} and $D = 2385$ kcal·Å^{10}·mol^{-1}. [c] The mixing rules are $\sigma_{ij} = (\sigma_{ii}\sigma_{jj})^{1/2}$ and $\epsilon_{ij} = (\epsilon_{ii}\epsilon_{jj})^{1/2}$. [d] The geometric parameters of the guanidinium ion are frozen to $r_{CN} = 1.321$ Å, $r_{NH} = 0.995$ Å, $\theta_{NCN} = 120.0°$, and $\theta_{HNH} = 117.1°$.

The PMFs have been obtained from MD free energy perturbation (FEP) simulations. The computational details and the models used in this paper are outlined in part 2. In part 3, we present an analysis of arginine pairs extracted from the Brookhaven protein data bank[17,18] (PDB), followed by the PMFs derived from the large-scale statistical simulations. The latter are compared to the work of Boudon et al. Next, a detailed comparison of the solvent structure between the contact ion pair and the solvent-separated ion pair, for the simulations with the SPC/E and the PSPC models, is proposed.

2. Models and Technical Details

A synthetic description of the different models considered is given in Table 1, and all the corresponding parameters are reported in Tables 2 and 3.

For the simulation with the TIP3P water model, the Gibbs module of the Amber 4.0 package was employed. The SHAKE[24,25] algorithm was used to constrain the bond lengths and angles of the ions to their equilibrium values. The partial charges were fitted to reproduce the electrostatic RHF/6−31G** potential created around the ion. Lennard-Jones parameters were taken from the Amber force field. We note that in the version of Amber that was utilized, a 10−12 hydrogen bond term was incorporated for the description of the H(ion)−O(water) interactions (i.e. $C = 7557$ kcal·Å^{12} /mol and $D = 2385$ kcal·Å^{10} /mol).

TABLE 3: Four-Site Polarizability Model of the Guanidinium Ion[a]

α^{CC}_{qq}	0.975	α^{CC}_{xx}	−0.098	$\alpha^{N_1N_1}_{xx}$	8.648
$\alpha^{N_iN_i}_{qq}$	0.952	α^{CC}_{yy}	1.140	$\alpha^{N_1N_1}_{yy}$	7.126
$\alpha^{CN_i}_{qq}$	−0.325	α^{CC}_{zz}	−0.087	$\alpha^{N_1N_1}_{zz}$	7.815
$\alpha^{N_iN_j}_{qq}$	−0.313				
$\alpha^{N_2N_2}_{xx}$	8.023	$\alpha^{N_3N_3}_{xx}$	8.023		
$\alpha^{N_2N_2}_{xz}$	0.361	$\alpha^{N_3N_3}_{xz}$	−0.361		
$\alpha^{N_2N_2}_{yy}$	7.126	$\alpha^{N_3N_3}_{yy}$	7.126		
$\alpha^{N_2N_2}_{zx}$	0.361	$\alpha^{N_3N_3}_{zx}$	−0.361		
$\alpha^{N_2N_2}_{zz}$	8.440	$\alpha^{N_3N_3}_{zz}$	8.440		

[a] The components are defined in the following molecular frame (all quantities are in au): C atom at $x = 0.0$, $y = 0.0$, $z = 0.0$; N_1 atom at $x = 0.0$, $y = 0.0$, $z = 2.497$; N_2 atom at $x = 2.162$, $y = 0.0$, $z = -1.248$; N_3 atom at $x = -2.162$, $y = 0.0$, $z = -1.248$. The total molecular dipolar polarizabilities recovered by this model are 36.41, 22.57, and 36.41 au for α_{xx}, α_{yy}, and α_{zz}, respectively. α_{qq} and α_{tt} denote the charge−charge and the dipole−dipole polarizabilities, respectively, with $t = x, y, z$.

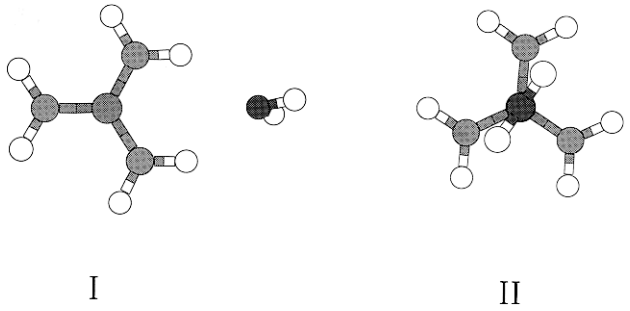

Figure 1. Two structures of the guanidinium−water complex obtained at the MP2/6-311++G** level: I is the global minimum (oxygen atom in the plane of the guanidinium ion), and II is a secondary minimum (oxygen atom above the carbon atom).

For the simulation with the SPC/E and the PSPC water models, we used the MDpol package.[26] This program allows to simulate condensed phases (e.g., bulks, mixtures, ionic solutions) using elaborate electrostatic models, in particular, models incorporating distributed polarizabilities.[27] Last, for the SPC/E simulation, the charges on the guanidinium ion were the same as in the simulation with the TIP3P water model (e.g., fitted to reproduce the RHF/6-31G** electrostatic potential) and the Lennard-Jones parameters were fitted to recover the structure and binding energy of the ion−water pair computed at the 6-31G(d) level by Boudon et al.

In the case of the simulation with a polarizable water model, new ab initio calculations at the second-order Møller−Plesset, MP2/6-311++G**, level were performed on the ion and the ion−water pair, for the two relative orientations shown in Figure 1, to obtain (i) improved electrostatic potential fitted atomic charges on the ion, and (ii) more accurate Lennard-Jones parameters. To fit the MP2/6-311++G** ion−water interaction energy correctly over large distances, the fitted charges were slightly scaled. All the Lennard-Jones parameters and partial charges characterizing the above models are given in Table 2.

The ions were considered as polarizable, using a model of distributed polarizabilities derived from the topological partitioning of electrostatic properties method.[28−30] This method makes use of Bader's atoms in molecules theory[31,32] in order to divide the molecular volume into disjoint regions centered around the nuclei. Choosing each of the nuclei as a center of

a multipole expansion for the charge density response function leads to multi-center multipolar polarizabilities, which include charge−flow terms (i.e. charge−charge and charge−multipole polarizabilities) as well as local and nonlocal atom−atom dipole−dipole (and higher) polarizabilities. In our case, we reduced the complexity of this model by choosing only the heavy atoms of the guanidinium ion as the centers for a multipole expansion up to the dipole terms, and relocalizing[33,34] all nonlocal charge−dipole and dipole−dipole terms to local C-atom and NH_2-group dipole polarizabilities. The charge density response function was calculated by means of the coupled perturbed Hartree−Fock (CPHF) theory, employing the polarizability optimized basis set of Sadlej,[35] in the RHF/6-31G** optimized geometry. This polarizability model (see Table 3) recovers in-plane and out-of-plane polarizabilities equal to 36.41 and 22.57 au, respectively, for the guanidinium ion.

The PMFs were computed with the free energy perturbation (FEP) method,[36] in which the free energy difference between two states, "0" and "1", is obtained from the following equation:

$$\Delta G = G_1 - G_0 = -RT \ln\langle e^{-(U_1-U_0)/RT}\rangle_0 \qquad (1)$$

Because the free energy difference for bringing the two ions from 2.5 to 8.0 Å is large, the total reaction path is divided into *N* contiguous substates connected by means of a coupling parameter, λ_i, which is related to the ion−ion distance, $r(\lambda)$, via

$$\Delta G = \sum_{i=1}^{N-1} \Delta G_i \qquad (2)$$

where ΔG_i is defined from (1) by

$$\Delta G_i = -RT \ln\langle e^{-(U_{\lambda_{i+1}}-U_{\lambda_i})/RT}\rangle_{\lambda_i} \qquad (3)$$

and:

$$r(\lambda_i) = r_0 + \lambda_i(r_1 - r_0) \qquad (4)$$

where r_0 and r_1 are the initial and the final values of the ion−ion distance and $0 \le \lambda_i \le 1$.

For the Amber/TIP3P simulation, 454 explicit water molecules and 2 ions were considered in a parallelepipedic box. The equations of motion were integrated with the isobaric−isothermal Berendsen algorithm,[37] and the SHAKE[24,25] procedure was used to constrain the ions to remain parallel. The fluctuating box length was ca. 24.0 Å, and the molecular cutoff distance set to 9.0 Å. The PMF was obtained by varying the ion−ion distance between 2.5 and 8.0 Å over 40 consecutive windows. In each window, 5 ps of equilibration were followed by 20 ps of data collection, with a time step equal to 1 fs.

The MDpol/SPC/E and MDpol/PSPC simulations were carried out in a similar manner. The two ions were immersed in a cubic box of length equal to 23.8 Å, containing 456 water molecules. A molecular cutoff distance corresponding to half of the box length was applied. The simulations were conducted in the NPT ensemble using the Nosé−Andersen algorithm,[38−40] modified to take into account the necessary holonomic constraints that maintain the ions rigid and parallel. All the simulations were carried out at 298 K and under 1 atm. Just like for the Amber/TIP3P simulation, the PMF was generated over 40 adjacent windows involving individually 5 ps of equilibration and 15 ps of data collection, i.e. 800 ps for each PMF, with a time step equal to 1 fs. These two simulations were performed on an IBM/SP2 machine. On this computer one MD step required 2 CPU seconds and 12 CPU seconds with the non-polarizable and the polarizable models, respectively.

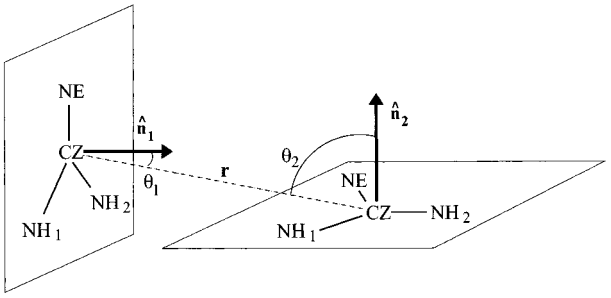

Figure 2. Definition of the geometrical descriptors used in the analysis of the relative orientation of the guanidinium ion pair found in the Brookhaven Protein Data Bank.

TABLE 4: Ab Initio MP2/6-311++G and Polarizable Model Optimized Structures of Water−Guanidinium Complexes for Two Particular Approaches (See Figure 1)**

structure	model	ab initio
I	-18.05 kcal·mol^{-1} $d_{C-O} = 3.32$ Å	-18.47 kcal·mol^{-1} $d_{C-O} = 3.36$ Å
II	-7.12 kcal·mol^{-1} $d_{C-O} = 2.96$ Å	-8.86 kcal·mol^{-1} $d_{C-O} = 2.91$ Å

3. Results and Discussion

3.1. Analysis of the Brookhaven Protein Data Bank. In their investigation of the Brookhaven protein data bank[17,18] (PDB), Magalhães et al.[16] have considered 41 proteins containing pairs of arginine residues, the C^ζ carbon atoms of which are separated by less than 5 Å. Here, we present an updated analysis carried out on 1680 non−redundant representative structures[41,42] of the PDB, from which 3561 pairs of arginine residues separated by 10 Å or less were extracted. In addition to the $C^\zeta-C^\zeta$ distance, we have examined the relative position of the two guanidinium moieties, by considering the angles, θ_1 and θ_2, formed by the normals to the plane of the cations, respectively $\hat{\mathbf{n}}_1$ and $\hat{\mathbf{n}}_2$, and the $\mathbf{C}^\zeta\mathbf{C}^\zeta$ vector (see Figure 2). Using these geometrical parameters, three distinct types of approach of the guanidinium ions can be defined: (i) a "stacked" approach, corresponding to $(\theta_1, \theta_2) < \theta_{limit}$ or $(\theta_1, \theta_2) \ge \pi - \theta_{limit}$, (ii) a "T-shaped" approach, corresponding to $\theta_1 < \theta_{limit}$ or $\theta_1 \ge \pi - \theta_{limit}$ and $\pi/2 - \theta_{limit} \le \theta_2 < \pi/2 + \theta_{limit}$, and its symmetric case, and, (iii) a planar approach, corresponding to $\pi/2 - \theta_{limit} \le (\theta_1, \theta_2) < \pi/2 + \theta_{limit}$ (where θ_{limit} denotes the aperture, such that $\theta_{limit} = 45°$ allows the entire space surrounding the cations to be explored). The latter will be referred in Table V to as approaches I, II, and III, respectively. Finally, the measure of the angle formed by the two $\mathbf{C}^\zeta\mathbf{N}^\epsilon$ vectors indicates whether the guanidinium ions have a relative parallel or antiparallel orientation.

As can be observed in Table 5, with an aperture of $\theta_{limit} = 45°$, there is a slight preference for parallel orientations, regardless of the $C^\zeta-C^\zeta$ distance. Interestingly enough, beyond ca. 13 Å of separation, the two orientations are equiprobable. It is noteworthy that, out of a subset of 1680 proteins, 125 pairs of arginine residues were found between 3 and 4 Å. Within this range, the "stacked" approach of the cations is predominant, and occurs when the two positively charged residues are exposed toward the aqueous medium, rather than buried in the interior of the protein. Hydration is, indeed, the *sine qua non* condition for obtaining thermodynamically stable contact interactions of the cations. As the arginine residues become more distant, however, the "T-shaped" population increases, but beyond 6

TABLE 5: Populations of the Three Types of Guanidinium−Guanidinium Approaches from an Analysis of the Brookhaven Protein Data Bank. The Definitions of the Descriptors Are Given in the Text

$C^\zeta-C^\zeta$	Gdm^+-Gdm^+ approach[a] I	II	III	parallel orientation	no. of pairs
		$\theta_{limit} = 45°$			
$3 \le r < 4$	0.768	0.184	0.048	0.592	125
$4 \le r < 5$	0.381	0.479	0.140	0.634	257
$5 \le r < 6$	0.094	0.460	0.446	0.626	372
$6 \le r < 7$	0.047	0.365	0.588	0.635	468
$7 \le r < 8$	0.108	0.345	0.547	0.609	563
$8 \le r < 9$	0.110	0.370	0.520	0.634	779
$9 \le r < 10$	0.072	0.402	0.526	0.578	997
		$\theta_{limit} = 10°$			
$3 \le r < 4$	1.000	0.000	0.000	0.333	3
$4 \le r < 5$	0.000	0.000	1.000	0.000	2
$5 \le r < 6$	0.000	0.000	1.000	0.333	3
$6 \le r < 7$	0.000	0.125	0.875	0.625	16
$7 \le r < 8$	0.000	0.143	0.857	0.500	14
$8 \le r < 9$	0.000	0.179	0.821	0.536	28
$9 \le r < 10$	0.000	0.056	0.944	0.444	36

[a] I, $(\theta_1, \theta_2) < \theta_{limit}$ or $(\theta_1, \theta_2) \ge \pi - \theta_{limit}$; II, $\theta_1 < \theta_{limit}$ or $\theta_1 \ge \pi - \theta_{limit}$ and $\pi/2 - \theta_{limit} \le \theta_2 < \pi/2 + \theta_{limit}$, and its symmetric case; III, $\pi/2 - \theta_{limit} \le (\theta_1, \theta_2) < \pi/2 + \theta_{limit}$.

Å, planar approaches are clearly preferred. This result is a priori surprising, since, on the basis of simple molecular mechanics minimizations of two guanidinium ions in vacuo, "T-shaped" approaches are always energetically more favorable than planar motifs. Whereas this statement holds for isolated guanidinium ions, it does not account for the presence of the rest of the arginine side chains, and, more generally, for the environment. The decrease of the aperture to $\theta_{limit} = 10°$, which corresponds to a more severe criterion for characterizing the approach of the guanidinium ions, leads to 102 pairs separated by 10 Å or less. The presence of only three "stacked" motifs, between 3 and 4 Å, suggests that, in most cases, the cations are not perfectly parallel, but rather tipped. We further note that, even between 4 and 6 Å, i.e. the expected separation for "T-shaped" structures, no such arrangements can be found. In fact, beyond 4 Å, mostly planar motifs are encountered.

Last, we underline that "stacked" arrangements of guanidinium moieties, that contribute to the stabilization of proteins, is not unique to those systems. In particular, the analysis of the Cambridge structural database (CSD)[43] reveals that, despite the reduced numbers of structures including pairs of guanidinium cations, face-to-face motifs are not marginal. In the pentaguanidinium (1- hydroxyethildenediphosphonato)hexaoxo-di-tungsten(VI) trihydrate,[44] for instance, carbon−carbon interatomic distances range between 3.4 and 4.3 Å.

3.2. Potentials of Mean Force. Boudon et al. have found, in the light of their MC/FEP simulation of two guanidinium ions in TIP4P water, that a contact ion pair at 3.3 Å was unusually stable. Their simulation involved 310 water molecules in a replicated parallelepipedic box with a cutoff at 8.5 Å. No relative orientational constraint was imposed on the approach of the ions, but, as already recognized in that study, it was not possible to sample uniformly all the relative orientations, and a nearly parallel approach was in fact observed.

In our study, rather than focusing on the important problem of finding the *true* PMF, we were mainly interested in the methodological question: to what extent is the PMF model-dependent? Is it sensitive to the explicit inclusion of induction effects? It was, thus, decided to enforce a parallel approach, under the assumption that, if a strong model-dependence is detected for this particular relative orientation, this means that the true PMF is also strongly model- dependent. Figure 3 shows

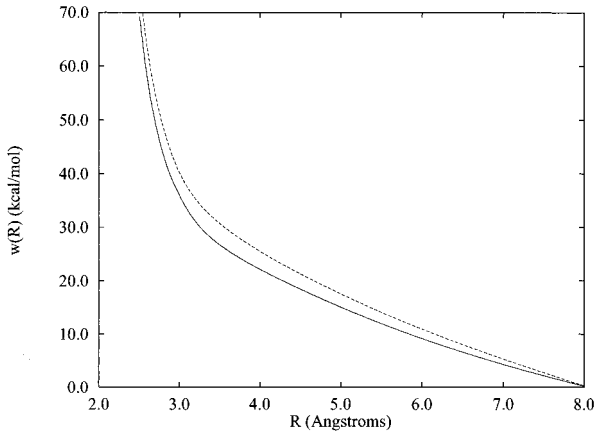

Figure 3. Gas-phase potential of mean force for the approach of two guanidinium ions constrained to remain parallel (solid line) and without any orientational constraint (dashed line), from MDpol/SPC/E simulation (see Tables 1 and 2).

the gas-phase PMF at 298 K for the MDpol/SPC/E model (i.e. the guanidinium pair interacting through charge−charge and Lennard-Jones interactions of the MDpol/SPC/E simulation) with and without constraint on the relative orientation. As can be observed, there are only minor differences between the two profiles.

The simulations with the SPC/E and the PSPC potentials were intended to provide additional insight into the effect of polarizability in PMF calculations. The two models differ, in fact, by more than the polarizability; not only the charges are different, but also the Lennard-Jones parameters, that were optimized, for both potential energy functions, to reproduce correctly thermodynamic properties of liquid water. We have tried to improve the force field by including explicitly induction forces, and refitting the guanidinium ion parameters to state-of-the-art ab initio calculations on the guanidinium ion and on the guanidinium−water complexes. The good structural and energetical features of the guanidinium−water complexes suggest that the two models are consistent. We further note that in the liquid phase, the solvation of one guanidinium ion is very similar for both models. Figure 4 depicts a series of atom−atom ion−water oxygen radial distribution functions (RDFs). They are also comparable for the two models, albeit a greater intensity is witnessed in the polarizable case. This is not surprising, since the deformability of the charge distribution in the polarizable case naturally favors an increase in the strength of the hydrogen bond formed by the water oxygen and the ion hydrogen atoms.

The ion−ion PMFs are given in Figure 5, and their characteristic points are reported in Table 6. Anchoring the PMF at 8.0 Å, the comparison of our PMFs with the one of Boudon et al. anchored at 5.5 Å is ambiguous. Nevertheless, for all three other models, the PMFs vary little beyond 5.5 Å (viz. within the 1 kcal·mol^{-1} range). It is anticipated that the 10 kcal·mol^{-1} stabilization of the contact ion pair (CIP) with TIP4P is more or less correct, provided that cutoff artifacts are not too important. The CIP is only stabilized by 6.7, 4.7, and 2.7 kcal·mol^{-1} for the TIP3P, SPC/E, and PSPC models, respectively, although the ion separation is much less model-dependent (3.3, 3.4, and 3.1 Å, respectively).

This observation relative to the effective water models can be compared to another well studied like-charge ion pair, namely the $Cl^-−Cl^-$ pair. Simulations have shown that the TIP4P water model predicts a very stable chloride−chloride CIP,[3] whereas simulations utilizing other effective potential functions such as SPC, SPC/E, the flexible SPC[45] and the polarizable Sprik's

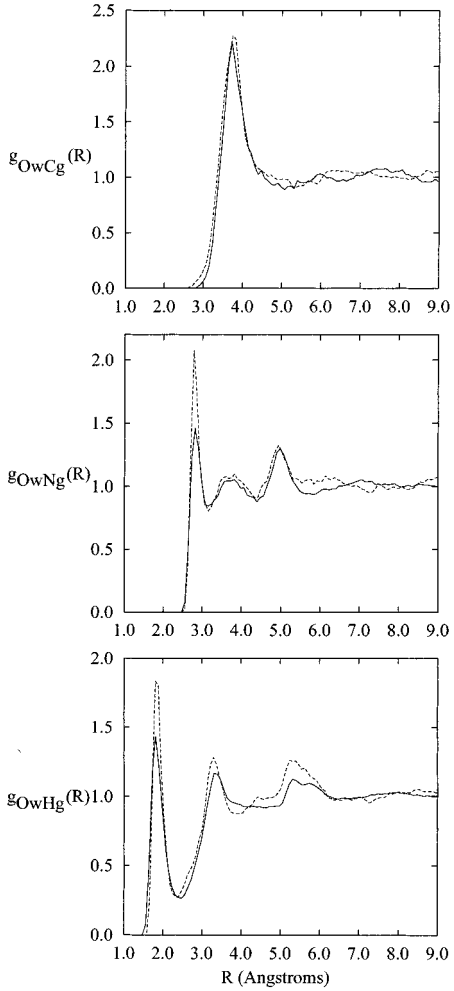

Figure 4. Some atom−atom water−guanidinium radial distribution functions obtained with SPC/E (solid line) and PSPC (dashed line) models. Ow, Cg, Ng, Hg represent the water oxygen, the guanidinium carbon, nitrogen, and hydrogen atoms, respectively.

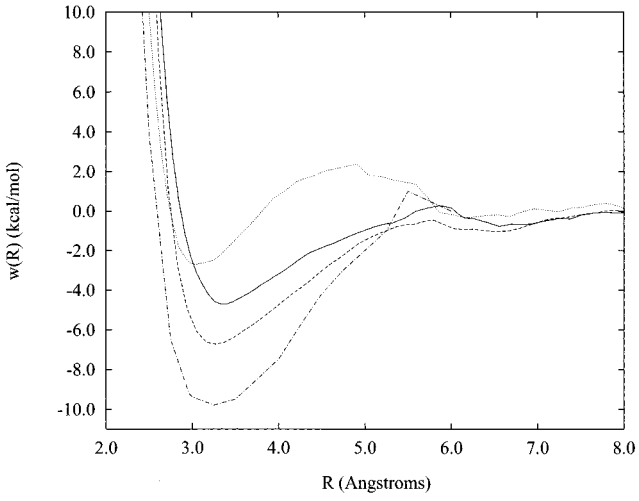

Figure 5. Potential of mean force for two guanidinium ions in water constrained to stay in parallel planes for three nonpolarizable water models (TIP4P, dashed dotted line; TIP3P, dashed line; SPC/E, solid line) and one polarizable model (PSPC, dotted line).

potential[46] do not share this feature. All these simulations tend to put forward the idea that TIP4P exaggerates the stability of like-charge ion pairs in an aqueous solution.

An important issue which has been addressed in a number of recent works is the influence of the cutoff on the PMF.[2,47−49] It has been shown in some particular cases[48−50] that the truncation of the interactions beyond a cutoff distance could lead to some artifacts. Because we were interested mainly in investigating the dependence of the PMF on the interaction potentials, it was chosen here to utilize a spherical cutoff to truncate long-range interactions. A more satisfactory approach would have been to consider lattice summation techniques. The condition that ensures a proper convergence of the sum, however, is the neutrality of the cell in which the simulation is carried out. This implies that one should either include counterions or a neutralizing background[51,52] to balance the net charge of the ion pair, albeit it is not clear how the free energy profile is affected by the introduction of this contribution. Another interesting issue, here, is the comparison of the SPC/E and the PSPC PMFs. Significant differences are observed, the CIP stability decreases from 4.7 to 2.7 kcal·mol^{-1}, although the barrier of dissociation remains close to 5.0 kcal·mol^{-1}. The solvent-separated ion pair (SSIP) minimum becomes very shallow and almost vanishes, which could be ascribed to insufficient sampling.

TABLE 6: Characteristic Points of the Potential of Mean Force Curves Given in Figure 5[a]

	CIP		DD			SSIP	
models	R	$W(R)$	R	$W(R)$	$\Delta W(R)$	R	$W(R)$
TIP4P	3.25	−9.80	5.50	1.00	10.80		
TIP3P	3.27	−6.73	5.80	−0.47	6.26	6.57	−1.03
SPC/E	3.39	−4.71	5.86	0.27	4.98	6.55	−0.77
PSPC	3.05	−2.70	4.90	2.38	5.08	6.20	−0.32

[a] CIP, DD, and SSIP denote the contact ion pair, the dissociation distance and the solvent-separated ion pair, respectively. $\Delta W(R)$ is the free energy difference between DD and CIP. Positions are in Å and energies in kcal·mol^{-1}.

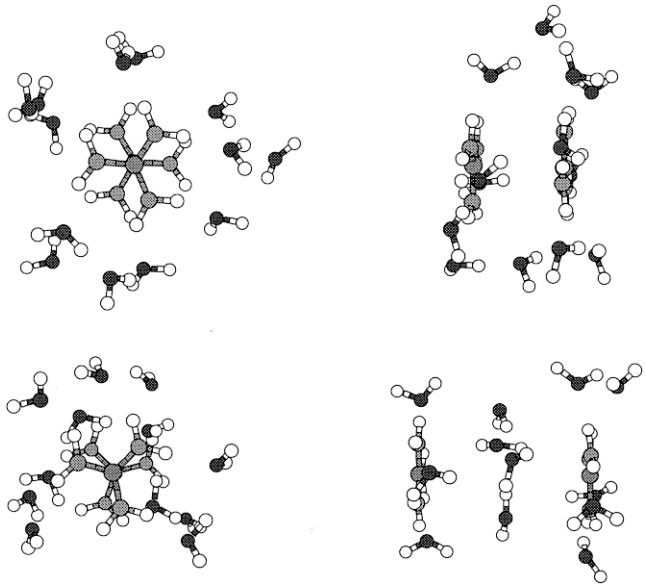

Figure 6. Typical configurations of the nearest solvent molecules surrounding the ion pair from the MDpol/SPC/E simulation. To the top, contact ion pair (d_{C-C} = 3.3 Å), to the bottom, solvent-separated ion pair (d_{C-C} = 6.5 Å).

3.3. Solvent Organization around the Ion Pair. To understand the differences observed between the PMFs obtained with polarizable and non-polarizable models, we have compared the solvent organization around the ion pair for the SPC/E and the PSPC cases. Two additional simulations were carried out, for each model, with a constraint imposed on the ion pair, so that the two guanidinium ions remain parallel at CIP and SSIP distances. Each simulation consists of 100 ps of MD trajectory using the systems that were equilibrated during the PMF

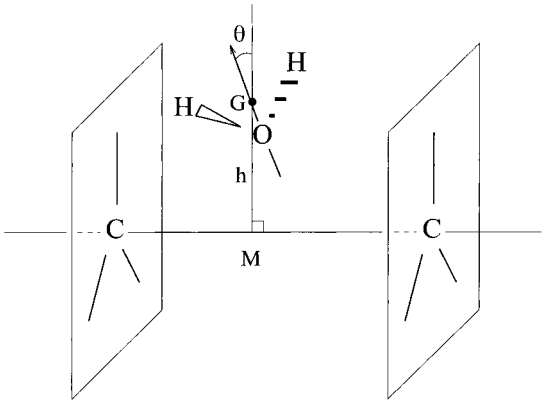

Figure 7. Definition of water organization descriptors in the region between both ion planes. h is the distance between the center of mass G of one water molecule and the point M on the C−C axis. θ is the angle between the water molecule permanent dipole and the **MG** vector.

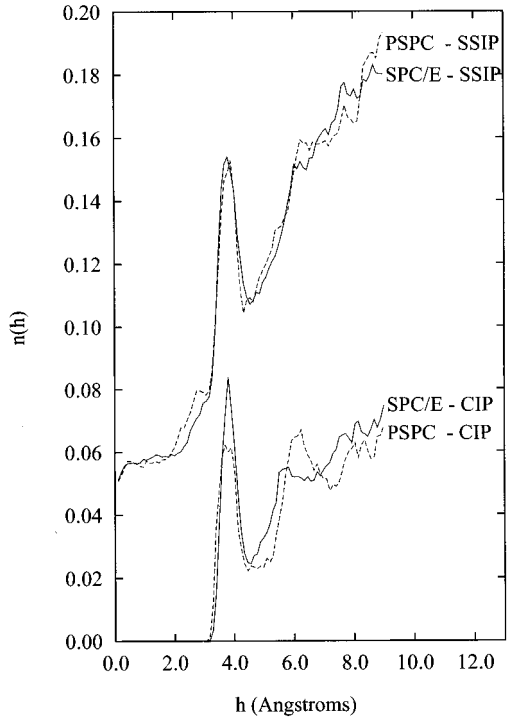

Figure 8. Distribution functions $n(h)$ of water molecules for contact and solvent separated ion pairs along a 100 ps MD simulation using SPC/E and PSPC models. SSIP curves have been shifted by 0.05.

calculations within the appropriate windows. The organization of the water is described using the quantities defined in Figure 7. Only the water molecules in a slab delimited by the two planes containing the ions were considered, and their orientations were described in terms of (i) the distance distribution functions, $n(h)$, between the center of mass G of the water molecules and the C−C axis, and (ii) the angular distribution functions, $n(\theta)$, between the permanent dipole and the vector **MG**.

Figure 8 shows the distance distribution functions, $n(h)$, in the four cases. The results obtained at SSIP distances (top) are very similar for both models, with a first peak centered at 3.8 Å. The integration of the first peak between 3 and 4 Å gives eight water molecules for both models. It is also clear that finding a water molecule in the region limited by the planes of the ions, i.e. near the C−C axis, corresponds to a rare event. At CIP distances, there are small differences between the two models, with a sharper first peak in the SPC/E case. The number of water molecules in the "h" range defined by this first peak are 4.8 and 5.1, for PSPC and SPC/E, respectively.

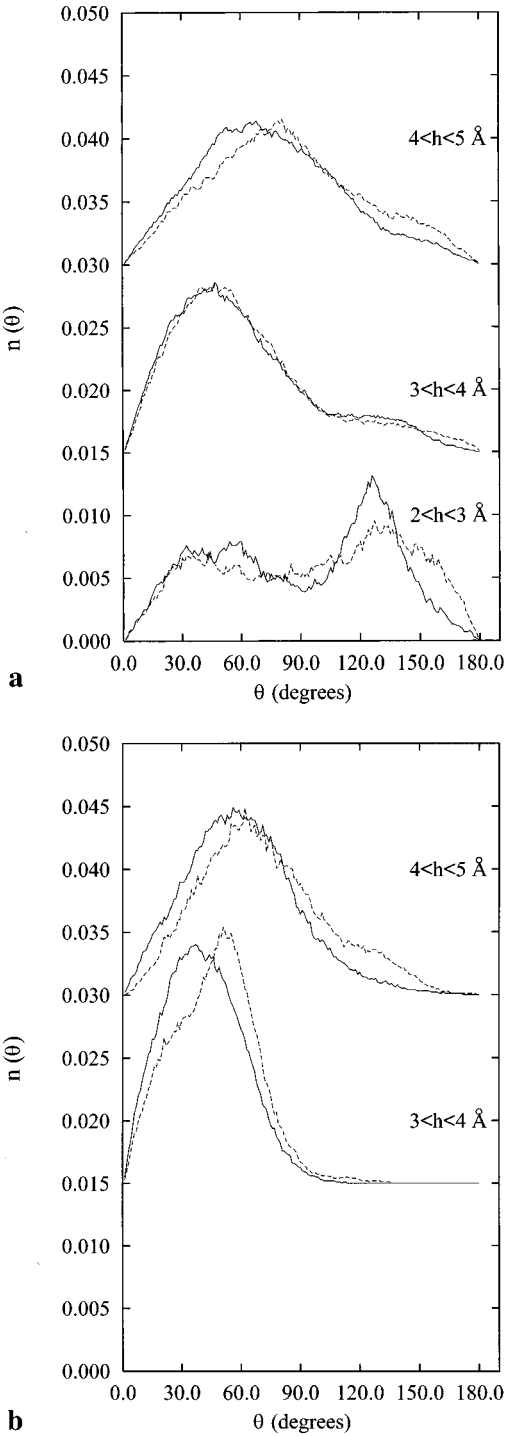

Figure 9. (a) Angular distribution functions $n(\theta)$ for different h ranges for solvent-separated ion pairs along a 100 ps MD simulation using SPC/E (solid line) and PSPC (dashed line) models. Curves corresponding to the range 3−4 and 4−5 Å have been shifted by 0.015 and 0.030, respectively. (b) Same as in (a) but for contact ion pairs.

The angular distribution functions, $n(\theta)$, are shown in Figure 9a,b, for SSIP and CIP distances, respectively. The "h" range between 3 and 4 Å is the most interesting, because it contains the main part of the first $n(h)$ peak. As has been observed previously, there is no difference between the SPC/E and the PSPC models at SSIP distances. We found a distribution function of the θ angle centered at 45°, whereas at CIP distances, there is a 20° deviation. In conclusion, it seems that there are no dramatic differences in the solvent structures around the ion pairs with the polarizable PSPC and the non-polarizable SPC/E water models.

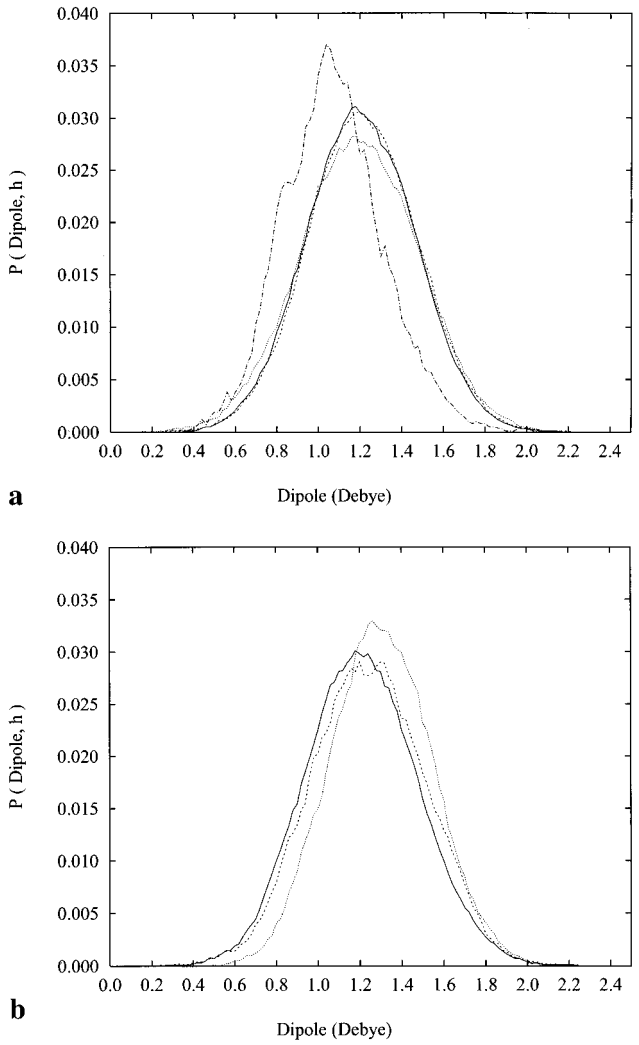

Figure 10. (a) Probability distribution of the induced dipole moment of the water molecules for various ranges of distances *h*. Results from a molecular dynamics simulation using the PSPC model with the guanidinium ion pair constrained at the SSIP distance (6.2 Å). Range 0−2 Å, dashed-dotted line; 2−4 Å, dotted line; 4−6 Å, dashed line; >6 Å, solid line. (b) Same as in (a) but with the guanidinium ion pair constrained at the CIP distance (3.05 Å).

The advantage of the polarizable model is to provide a realistic description of the polarization of the solvent in the vicinity of the ions. It was, thus, interesting to examine the polarization of the water molecules with respect to their distances from the ion pair. We show, in Figure 10a,b, the probability distributions of the induced dipole of the water molecules for various ranges of the distance "*h*". In the SSIP case (see Figure 10a), we find in the 0−2 Å range an induced dipole of about 0.15 D lower than those of the water molecules beyond 2 Å. In the CIP case, the water molecules present in the 2−4 and 4−6 Å ranges are, respectively, more polarized by about 0.06 and 0.14 D than in the bulk (i.e., >6 Å). This result was expected, but reminds that, even for large ions with a delocalized unit charge, taking into account polarization effects is of crucial importance. This remark is of increasing importance as the charge increases and becomes more localized, (e.g., Fe^{2+} or Fe^{3+} cations).

4. Conclusions

We have presented in this study the PMFs characterizing the constrained approach of two rigid guanidinium ions in liquid water, at infinite dilution, using MD/FEP methodology. This chemical system constitutes a case example of ionic association in liquid water. Moreover, guanidinium ions represent an appropriate model to study the association of arginine side chains that have been observed in proteins.[15] This specific interaction appears to contribute to the stability of several proteins, as has been demonstrated by our analysis of the PDB on 1680 representative structures.

The definition of the potential energy functions, and, in particular, the treatment of polarization effects, is of paramount importance. On one hand, polarization effects can be described in an average manner. On the other hand, their explicit treatment guarantees the transferability of the potential energy functions from the gas phase to the liquid phase and, at the same time, constitutes a refinement in the description of the intermolecular interactions. To verify this point, various intermolecular potentials, ranging from commercially available force fields to newly developed ab initio-based polarizable potentials have been utilized. The PMF for ion association has been found to be very sensitive to the model employed. The TIP4P effective model seems to overestimate the stability of the contact ion pair with respect to other effective models, like TIP3P or SPC/E. All models, however, confirm the stability of the guanidinium-guanidinium contact ion pair in an aqueous solution at about 3.0−3.5 Å.

The quantitative effect of both the parameters of the model and polarizability underlines once again the necessity of treating the predominant interactions in ion-solvent systems, i.e., electrostatic and induction, as accurately as possible. Such a requirement is obviously not sufficient to obtain reliable results that can be compared satisfactorily to experimental data—the correct treatment of long-range electrostatic interactions and the removal of orientational constraints while approaching the two cations are still two important issues to be addressed. Together with the explicit inclusion of polarizability effects, these features contribute to a significant increase in computer time, thereby precluding, for the time being, this kind of simulation to be carried out routinely. Nevertheless, alternative algorithms, like the extended Lagrangian[53] approach, constitute an efficient way for incorporating polarizability effects into molecular simulations.

References and Notes

(1) Jorgensen, W. L.; Buckner, J. K.; Huston, S. E.; Rossky, P. J. *J. Am. Chem. Soc.* **1987**, *109*, 1891.
(2) Huston, S. E.; Rossky, P. J. *J. Phys. Chem.* **1989**, *93*, 7888.
(3) Buckner, J. K.; Jorgensen, W. L. *J. Am. Chem. Soc.* **1989**, *111*, 2507.
(4) Sesé, G.; Guàrdia, E.; Padró, J. A. *J. Phys. Chem.* **1995**, *99*, 12647.
(5) Belch, A. C.; Berkowitz, M.; McCammon, J. A. *J. Am. Chem. Soc.* **1986**, *108*, 1755.
(6) Dang, L. X.; Pettitt, B. M. *J. Am. Chem. Soc.* **1987**, *109*, 5531.
(7) Guàrdia, E.; Rey, R.; Padró, J. A. *Chem. Phys.* **1991**, *155*, 187.
(8) Karim, O. A.; McCammon, J. A., *J. Am. Chem. Soc.* **1986**, *108*, 1762.
(9) Smith, D. E.; Dang, L. X. *J. Chem. Phys.* **1994**, *100*, 3757.
(10) Pettitt, B. M.; Rossky, P. J. *J. Chem. Phys.* **1986**, *84*, 5836.
(11) Dang, L. X.; Pettitt, B. M. *J. Phys. Chem.* **1990**, *94*, 4303.
(12) Hummer, G.; Soumpasis, D. M.; Neumann, M. *Mol. Phys.* **1993**, *81*, 1155.
(13) van Belle, D.; Wodak, S. J. *J. Am. Chem. Soc.* **1993**, *115*, 647.
(14) New, M. H.; Berne, B. J. *J. Am. Chem. Soc.* **1995**, *117*, 7172.
(15) Mrabet, N. T.; van den Broeck, A.; van den Brande, I.; Stanssens, P.; Laroche, Y.; Lambeir, A. M.; Matthijssens, G.; Jenkins, J.; Chiadmi, M.; van Tilbeurgh, H.; Rey, F.; Janin, J.; Quax, W. J.; Lasters, I.; De Maeyer, M.; Wodak, S. J. *Biochemistry* **1992**, *31*, 2239.
(16) Magalhães, A.; Maigret, B.; Hoflack, J.; Gomes, J. A. N. F.; Scheraga, H. A. *J. Protein Chem.* **1994**, *13*, 195.
(17) Bernstein, F. C.; Koetzle, T. F.; Williams, G. J. B; Mayer, G. F.; Brice, M. D.; Rodgers, M. D.; Kennard, O.; Shimanouchi, T.; Tasumi, M. *J. Mol. Biol.* **1977**, *112*, 535.
(18) Abola, E. E.; Bernstein, F. C.; Bryant, S. H.; Koetzle, T. F.; Weng, J. In *Crystallographic Databases-Information Content, Software Systems,*

Scientific Application; Allen, F., Sievers, R., Eds.; Data Commission of the International Union of Crystallography: Bonn/Cambridge/Chester, 1978; p 107.
(19) Boudon, S.; Wipff, G.; Maigret, B. *J. Phys. Chem.* **1990**, *94*, 6056.
(20) Jorgensen, W. L.; Chandrasekhar, J.; Madura, J. D.; Impey, R. W.; Klein, M. L. *J. Chem. Phys.* **1983**, *79*, 926.
(21) Berendsen, H. J. C.; Grigera, J. R.; Straatsma, T. P. *J. Phys. Chem.* **1987**, *91*, 6269.
(22) Ahlström, P.; Wallqvist, A.; Engström, S.; Jönsson, B. *Mol. Phys.* **1989**, *68*, 563.
(23) Berendsen, H. J. C.; Postma, J. P. M.; van Gunsteren, W. F.; Hermans, J., *Intermolecular Forces*; Pullman, B., Ed.; Reidel: Dordrecht, 1981.
(24) Ryckaert, J.; Cicotti, G.; Berendsen, H. J. C. *J. Comput. Phys.* **1977**, *23*, 327.
(25) van Gunsteren, W. F.; Berendsen, H. J. C. *Mol. Phys.* **1977**, *34*, 1311.
(26) Soetens, J. C. Thesis, UniversitéHenri Poincaré-Nancy I, 1996.
(27) Soetens, J. C.; Millot, C. *Chem. Phys. Lett.* **1995**, *235*, 22.
(28) Ángyán, J. G.; Jansen, G.; Loos, M.; Hättig, C.; Hess, B. A. *Chem. Phys. Lett.* **1994**, *219*, 267.
(29) Jansen, G.; Hättig, C.; Hess, B. A.; Ángyán, J. G. *Mol. Phys.* **1996**, *88*, 69.
(30) Hättig, C.; Jansen, G.; Hess, B. A.; Ángyán, J. G. *Mol. Phys.* **1997**, *91*, 145.
(31) Bader, R. F. W. *Atoms in Molecules−A Quantum Theory*; Oxford University Press: London, 1990.
(32) Bader, R. F. W. *Chem. Rev.* **1991**, *91*, 893.
(33) Hättig, C.; Jansen, G.; Hess, B. A.; Ángyán, J. G. *Can. J. Chem.* **1996**, *74*, 976.
(34) Stone, A. J.; Hättig, C.; Jansen, G.; Ángyán, J. G. *Mol. Phys.* **1996**, *89*, 592.
(35) Sadlej, A. J. *Czech Chem. Commun.* **1988**, *53*, 1995.
(36) Zwanzig, R. W. *J. Chem. Phys.* **1954**, *22*, 1420.
(37) Berendsen, H. J. C.; Postma, J. P. M.; van Gunsteren, W. F.; DiNola, A.; Haak, J. R. *J. Chem. Phys.* **1984**, *81*, 3684.
(38) Nosé, S. *Mol. Phys.* **1984**, *52*, 255.
(39) Nosé, S. *J. Chem. Phys.* **1984**, *81*, 511.
(40) Andersen, H. C. *J. Chem. Phys.* **1980**, *72*, 2384.
(41) Hobohm, U.; Scharf, M.; Schneider, R.; Sander, C. *Protein Sci.* **1992**, *1*, 409.
(42) Hobohm, U.; Sander, C. *Protein Sci.* **1994**, *3*, 522.
(43) Allen, F. H.; Davies, J. E.; Johnson, O. J.; Kennard, O.; Macrae, C. F.; Mitchell, E. M.; Mitchell, G. F.; Smith, J. M.; Watson, D. G. *J. Chem. Inf. Comput. Sci.* **1991**, *31*, 187.
(44) Sergienko, V. S.; Tolkacheva, A. B. *Zh. Neorg. Khim.* **1994**, *39*, 243.
(45) Guàrdia, E.; Rey, R.; Padró, J. A. *J. Chem. Phys.* **1991**, *95*, 2823.
(46) Karim, O. A. *J. Chem. Phys.* **1992**, *96*, 9237.
(47) Dang, L. X.; Pettitt, B. M.; Rossky, P. J. *J. Chem. Phys.* **1992**, *96*, 4046.
(48) Bader, J. S.; Chandler, D. *J. Phys. Chem.* **1992**, *96*, 6423.
(49) Auffinger, P.; Beveridge, D. L. *Chem. Phys. Lett.* **1995**, *234*, 413.
(50) Del Buono, G. S.; Figueirido, F. E.; Levy, R. M. *Chem. Phys. Lett.* **1996**, *263*, 521.
(51) Roberts, J. E.; Schnitker, J. *J. Chem. Phys.* **1994**, *101*, 5024.
(52) Roberts, J. E.; Schnitker, J. *J. Phys. Chem.* **1995**, *99*, 1322.
(53) Sprik, M.; Klein, M. L. *J. Chem. Phys.* **1988**, *89*, 7556.